Ultra-high sensitive acetylene detection using quartz-enhanced photoacoustic spectroscopy with a fiber amplified diode laser and a 30.72 kHz quartz tuning fork

Yufei Ma,[1,2,a)] Ying He,[1] Ligong Zhang,[1] Xin Yu,[1] Jingbo Zhang,[1] Rui Sun,[2] and Frank K. Tittel[3]
[1]*National Key Laboratory of Science and Technology on Tunable Laser, Harbin Institute of Technology, Harbin 150001, China*
[2]*Post-doctoral Mobile Station of Power Engineering and Engineering Thermophysics, Harbin Institute of Technology, Harbin 150001, China*
[3]*Department of Electrical and Computer Engineering, Rice University, 6100 Main Street, Houston, Texas 77005, USA*

(Received 26 September 2016; accepted 9 January 2017; published online 18 January 2017)

An ultra-high sensitive acetylene (C_2H_2) Quartz-enhanced photoacoustic spectroscopy (QEPAS) sensor based on a high power laser and a quartz tuning fork with a resonance frequency f_0 of 30.72 kHz was demonstrated. An erbium-doped fiber amplifier (EDFA) amplified distributed feedback diode laser with a center wavelength of 1.53 μm was used as the exciting source. A 33.2 ppb minimum detection limit (MDL) at 6534.37 cm^{-1} was achieved, and the calculated normalized noise equivalent absorption coefficient was 3.54×10^{-8} cm^{-1} W/$\sqrt{Hz}$ when the laser output power was 1500 mW. The ppb-level detection sensitivity of C_2H_2 validated the reported QEPAS method. *Published by AIP Publishing.* [http://dx.doi.org/10.1063/1.4974483]

The quartz-enhanced photoacoustic spectroscopy (QEPAS) technique is one of the most promising ways for trace gas sensing.[1] In QEPAS technology, a low cost, commercially available mm sized piezoelectric quartz tuning fork (QTF) is used as an acoustic wave transducer, and the acoustic energy is accumulated in the sharply resonant QTF.[2,3] QEPAS has been applied to many trace gas detection applications due to its significant advantages such as high sensitivity, selectivity, and compactness.[4–13] The primary QEPAS noise source is Johnson thermal noise of the QTF. The QEPAS signal amplitude S is given by Equation (1)[14]

$$S \propto \frac{\alpha P Q}{f_0}, \tag{1}$$

where α is the absorption coefficient, P is the optical power, Q is the Q-factor of QTF, and f_0 is the QTF resonance frequency. One of the main QEPAS development goals is how to increase the QEPAS signal amplitude.

An important advantage of QEPAS is that the performance of QEPAS-based sensors can be improved when the excitation laser power is increased, since the QEPAS detection sensitivity scales linearly with excitation laser power P, as seen in Eq. (1). This feature differs from other laser absorption spectroscopy techniques such as tunable diode laser absorption spectroscopy (TDLAS).[15] Diode lasers are usually used in QEPAS based sensing systems due to their compactness and low cost. However, the output power of diode lasers is in the range of several milliwatts, which limits the QEPAS detection performance. Optical fiber amplifiers, which are widely used in optical communications, can realize significant optical signal amplification. In a commercially available optical fiber amplifier, a short length of single-mode optical fiber is doped with rare-earth ions and is pumped by diode lasers. Erbium-doped fiber amplifiers (EDFAs) offer several advantages, such as high gain, low noise, polarization independence, and fiber compatibility.[16,17] An EDFA can be used to achieve amplification gain of more than 30 dB when an appropriate seed diode laser is injected. Three operating wavelength bands (S band: 1450–1550 nm, C band: 1520–1570 nm, and L band: 1565–1610 nm) are commercially available. However, the beam quality and linewidth of the EDFA output should be considered in the QEPAS technique because the noise level of the QEPAS sensor is related to them. In 2015, a QEPAS-based H_2S sensor using an EDFA was reported by Wu *et al.*[18,19] Due to the limited output performance of the EDFA, the noise amplitude of this sensor was large. In order to reduce the noise level, an electrical modulation cancellation method (E-MOCAM)[18] and a custom QTF with a large prong spacing[19] were used in these investigations, respectively, which resulted in a complex sensor system with a higher cost.

It can be further seen from Eq. (1) that the QEPAS sensor signal is inversely proportional to the QTF resonance frequency. This feature is due to the fact that a QTF with a smaller f_0 will result in a longer effective integration time, which increases the QEPAS signal. In QEPAS, commercially available QTFs with a f_0 of ~32.76 kHz are typically employed, but since 2013, the use of custom QTFs in QEPAS based sensor systems capable of ppb concentration levels' detection sensitivity was reported.[20]

In this paper, an ultra-high sensitive acetylene (C_2H_2) QEPAS sensor based on a high power diode laser source and a low resonance frequency QTF was demonstrated. An EDFA amplified distributed feedback (DFB) diode laser, which combines the merits of an EDFA and a diode laser emitting at 1.53 μm with superior output performance, was used as the laser excitation source. A QTF with f_0 of 30.72 kHz was

a)Electronic mail: mayufei926@163.com

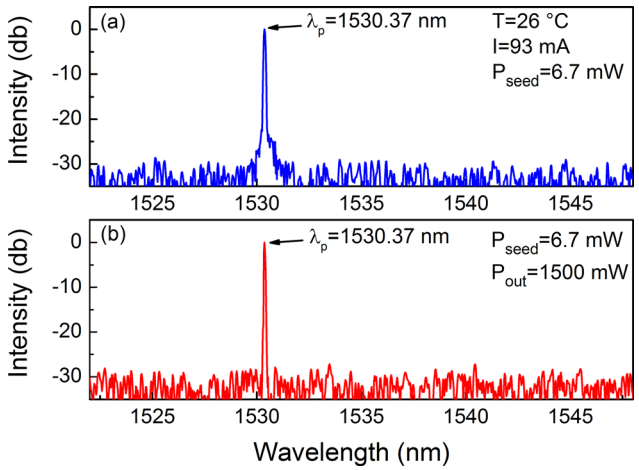

FIG. 1. Diode laser emission spectrum. (a) Seed diode laser with a 6.7 mW output power. (b) EDFA amplified diode laser with a 1500 mW output power.

employed as an acoustic wave transducer. C_2H_2 was chosen as the analyte due to its important applications in the detection of fault gases in transformers[21] and in ethylene streams for polyethylene production.[22]

A pigtailed, near infrared, continuous wave (CW), DFB diode laser emitting at 1.53 μm was employed as the excitation source. The DFB diode laser was mounted in a 14-pin butterfly package that included a thermoelectric controller (TEC). A 1530.37 nm (6534.37 cm^{-1}) absorption line was selected as one of the strongest lines in the 1.53 μm spectral range for C_2H_2 detection using the HITRAN 2012 data base. This absorption line is free from spectral interference of other molecules. The output wavelength of the diode laser can target the 1530.37 nm absorption line by controlling the temperature of the TEC and the injection current. This was accomplished by setting the diode laser temperature and current to 26 °C and 93 mA, respectively. The optical output power was 6.7 mW in this case as recorded by an optical power meter (Model No. PS19Q, Coherent) and the emission spectrum was measured by a laser wavelength meter with a resolution of 0.2 pm (Model No. 721A, Bristol) as shown in Fig. 1(a). The signal-to-noise ratio is >30 dB. The output of the diode laser was sent to the EDFA for power amplification. The EDFA offers an adjustable output power from 50 mW to 1500 mW at the same wavelength as the seed laser. The EDFA consisted of both a preamplifier and a power amplifier for power scaling. Erbium (Er^{3+})-ytterbium (Yb^{3+}) co-doped fiber was used in the EDFA in order to increase the pumping efficiency. Er^{3+} was efficiently sensitized by adding Yb^{3+} doping. Amplified spontaneous emission (ASE) of the gain fiber must be minimized in order to reduce the noise level of the amplified diode laser. This was accomplished by means of a narrow-band filter with a bandwidth of 1 nm and a center wavelength of 1530.33 nm. The output spectrum of the amplified laser and the EDFA is shown in Figs. 1(b) and 2(a), respectively. From Fig. 1(b), it can be seen that with a 6.7 mW input, the EDFA amplified laser output power of 1500 mW with a signal-to-noise ratio of ~30 dB was obtained. From Figs. 1(a) and 1(b), it can be seen that the linewidth of the amplified diode laser was compressed when compared with the seed laser. This is due to the fact that a high power intensity is beneficial to achieve a high gain; therefore, the seed laser with wavelength close to the peak of 1530.37 nm can obtain a more obvious amplification. A narrower linewidth means a better spectral resolution and is therefore advantageous for improving the selectivity and reducing the noise level of the reported C_2H_2 sensor.

A schematic of the QEPAS based sensor platform is shown in Fig. 2. An opto-isolator in the EDFA was used to protect the DFB laser against back reflections. The output laser beam from the opto-isolator was collimated by using a fiber collimator (FC) and subsequently focused between the QTF prongs inside an acoustic detection module (ADM) by means of a plano-convex CaF_2 lens (L) with a 40 mm focal length. After passing through the ADM, the diode laser beam was directed to an optical power meter, which is used for alignment verification of the QEPAS based sensor system. A QTF with f_0 of 30.72 kHz was employed as the acoustic transducer. Wavelength modulation spectroscopy (WMS) with 2nd harmonic detection was utilized for sensitive C_2H_2 concentration measurements. Modulation of the laser current was performed by applying a sinusoidal modulation to the direct current ramp of the diode laser at half of the QTF resonance frequency ($f = f_0/2 \approx 15.36$ kHz). The piezoelectric signal generated by the QTF was detected by a low noise transimpedance amplifier (TA) with a 10 MΩ feedback resistor and converted into a voltage, which was transferred to a

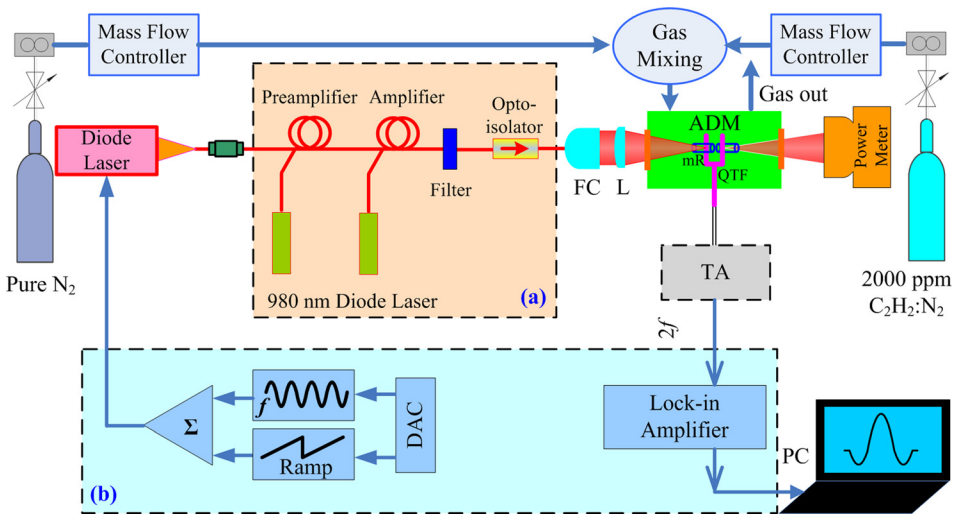

FIG. 2. Schematic of a C_2H_2-QEPAS sensor. (a) EDFA. (b) Control electronics for modulation and demodulation. FC: fiber collimator; L: plano-convex lens; ADM: acoustic detection module; mR: micro-resonator; and TA: transimpedance amplifier.

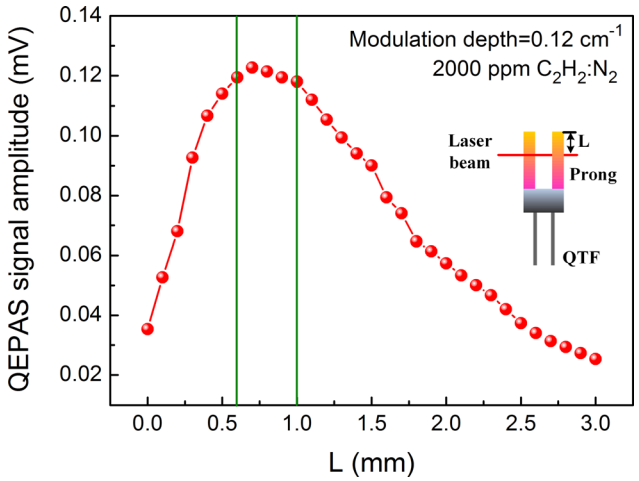

FIG. 3. C_2H_2-QEPAS signal amplitude as a function of L at a modulation depth of 0.12 cm^{-1}.

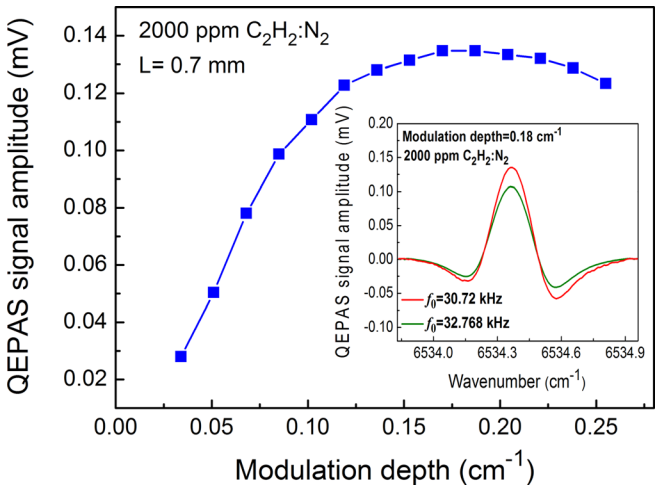

FIG. 4. C_2H_2-QEPAS signal amplitude as a function of modulation depth.

lock-in amplifier for demodulation. The control electronic components required for modulation and demodulation are shown in Fig. 2(b). The C_2H_2-QEPAS sensor performance was evaluated at different C_2H_2 concentration levels. Two mass flow controllers with a mass flow uncertainty of 3% were used to dilute 2000 ppmv (parts in 10^6 by volume) C_2H_2 in nitrogen (N_2). The measurements were carried out at atmospheric pressure and room temperature.

The QEPAS sensor performance using a diode laser without EDFA was evaluated first. A certified mixture of 2000 ppm C_2H_2:N_2 was used. The influence of distance (L) between the diode laser beam and the top of QTF prongs on the QEPAS signal level was investigated, and the experimental results are shown in Fig. 3. An inset in Fig. 3 displays the diode laser beam, the QTF, and the parameter L. The modulation depth of the laser wavelength was set to 0.12 cm^{-1}. The 2*f* C_2H_2-QEPAS signal amplitude increased rapidly with L, when L was <0.6 mm. The peak of the 2*f* signal amplitude occurred in the range of L from 0.6 mm to 1 mm. With a further increase of L, the signal amplitude decreased due to the more challenging QTF prong vibrations when the acoustic wave source is at the bottom of the QTF prongs. In the following experiments, an optimum value for L of 0.7 mm was chosen to achieve the maximum QEPAS signal amplitude.

The laser wavelength modulation depth was optimized in order to improve the 2*f* QEPAS signal amplitude. The dependence of the QEPAS signal amplitude as a function of the laser wavelength modulation depth for a 2000 ppm C_2H_2:N_2 mixture is shown in Fig. 4. The QEPAS signal amplitude increased with the modulation depth, but when the modulation depth was >0.18 cm^{-1}, the signal amplitude started to decrease. Therefore, a modulation depth of 0.18 cm^{-1} was found to be the optimum value. A comparison was made to confirm the advantages of using a QTF with a f_0 of 30.72 kHz when compared with a standard QTF with a f_0 of 32.768 kHz. The experiments were carried out for the same conditions, and the results are displayed in the inset of Fig. 4. We found that, compared to a QTF with f_0 of 32.768 kHz, the QEPAS signal increased 1.3 times when a QTF with f_0 of 30.72 kHz was used. Two aspects contributed to this QEPAS signal increase. One is a lower f_0 of 30.72 kHz. The other is an increased Q factor. The Q factor for the 32.768 kHz QTF was 7693 and that for the 30.72 kHz QTF was 9746.

The QEPAS sensor performance was further investigated using EDFA amplified DFB diode laser excitation. The optical power of the amplified diode laser increased from 100 mW to 1500 mW. The QEPAS sensor signal amplitude as a function of diode laser optical power is shown in Figs. 5(a) and 5(b). From Fig. 5(a), it can be seen that the QEPAS signal amplitude improved with increasing laser optical power. The peak values of QEPAS signal are depicted in Fig. 5(b) and a linear fitting procedure was implemented. The calculated R-square value is equal to ~0.99. This implies that the sensor system exhibits an excellent linearity response of optical power levels. No saturable absorption effects were observed. This means that the C_2H_2-QEPAS signal amplitude can be even further improved when a higher power EDFA will be used.

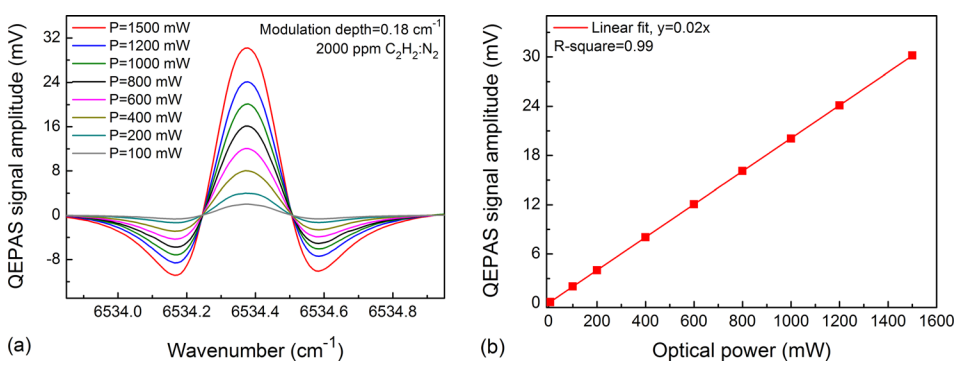

FIG. 5. QEPAS signal amplitude. (a) Different optical power levels with a modulation depth of 0.18 cm^{-1}. (b) QEPAS signals amplitude from (a) as a function of optical power.

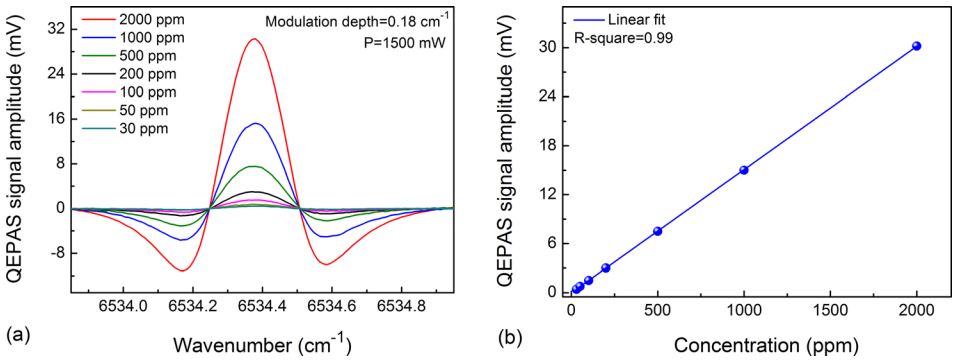

FIG. 6. QEPAS signal amplitude. (a) Different C_2H_2 concentration levels with a modulation depth of $0.18\,cm^{-1}$. (b) QEPAS signal amplitude from Fig. 6(a) as a function of C_2H_2 concentrations.

To verify the linear concentration response of the QEPAS based C_2H_2 sensor platform, the 2000 ppm C_2H_2:N_2 gas mixture was diluted with dry N_2 down to 30 ppm C_2H_2 concentration levels (see Fig. 6(a)). The measured QEPAS signal amplitude as a function of C_2H_2 concentrations is plotted in Fig. 6(b). The calculated R-square value is equal to ~0.99 after a linear fitting procedure, which indicates that the sensor system has an excellent linearity response of the C_2H_2 concentration levels.

A significant enhancement of the QEPAS signal can be achieved when two metallic tubes acting as a micro-resonator (mR) are added to the QTF sensor architecture.[23] The length and inner diameter of stainless tubes were selected to be 4 mm and 0.5 mm, respectively, to constitute the mR. A 200 ppm C_2H_2:N_2 mixture was used to avoid signal saturation of the custom made lock-in amplifier. The measured 2*f* QEPAS signals with and without mR at a modulation depth of $0.18\,cm^{-1}$ are shown in Fig. 7(a). The QEPAS signal was enhanced ~8 times as a result of the addition of the two mR tubes. Fig. 7(b) depicts the background signal measured when the ADM was flushed with ultra high purity N_2. The background signal was 4.15 μV. The 1σ minimum detection limit (MDL) of the C_2H_2-QEPAS sensor was 33.2 ppbv for a 1 s time constant of the lock-in amplifier based on the data depicted in Fig. 7. The calculated normalized noise equivalent absorption coefficient (NNEA) was $3.54 \times 10^{-8}\,cm^{-1}\,W/\sqrt{Hz}$ based on the optical power of 1500 mW.

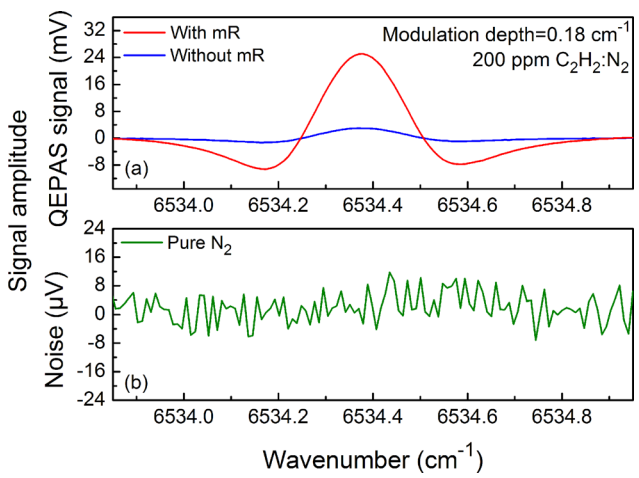

FIG. 7. Signal amplitude. (a) QEPAS signal with and without a mR. (b) Pure N_2 for a noise background determination. mR: micro-resonator.

In conclusion, an ultra-high sensitive QEPAS based C_2H_2 sensor was demonstrated. An EDFA amplified diode laser with an output optical power up to 1500 mW was used as the QEPAS excitation source. A QTF with a low f_0 of 30.72 kHz was employed as an acoustic wave transducer. The high laser power and the low resonance frequency of QTF increase the QEPAS signal level. A significant further signal enhancement of 8 times was obtained when a mR was added to the QTF sensor architecture. For the C_2H_2 sensor system operating at atmospheric pressure, a 33.2 ppb MDL at $6534.37\,cm^{-1}$ was achieved when the modulation depth and data acquisition time of the lock-in amplifier were set to $0.18\,cm^{-1}$ and 1 s, respectively. The ppb-level detection sensitivity verified that the design of the reported QEPAS method demonstrated a significantly enhanced sensor system performance. The sensor capability can be further improved when an EDFA with even higher output power and a QTF with a lower f_0 are used.

This work was supported by the National Natural Science Foundation of China (Grant No. 61505041), the Natural Science Foundation of Heilongjiang Province of China (Grant No. F2015011), the General Financial Grant from the China Postdoctoral Science Foundation (Grant No. 2014M560262), the Special Financial Grant from the China Postdoctoral Science Foundation (Grant No. 2015T80350), the Special Financial Grant from the Heilongjiang Province Postdoctoral Foundation (Grant No. LBH-TZ0602), the Postdoctoral Fund of Heilongjiang Province (Grant No. LBH-Z14074), the Fundamental Research Funds for the Central Universities (Grant No. HIT. NSRIF. 2015044), the Application Technology Research and Development Projects of Harbin (No. 2016RAQXJ140), the National Key Scientific Instrument and Equipment Development Projects of China (Grant No. 2012YQ040164). Frank K. Tittel acknowledges the financial support from the U.S. National Science Foundation ERC MIRTHE award and a grant C-0586 from the Welch Foundation.

[1]A. A. Kosterev, Y. A. Bakhirkin, R. F. Curl, and F. K. Tittel, Opt. Lett. **27**, 1902 (2002).
[2]Y. F. Ma, X. Yu, G. Yu, X. D. Li, J. B. Zhang, D. Y. Chen, R. Sun, and F. K. Tittel, Appl. Phys. Lett. **107**, 021106 (2015).
[3]P. Patimisco, G. Scamarcio, F. K. Tittel, and V. Spagnolo, Sensors **14**, 6165 (2014).
[4]H. M. Yi, R. Maamary, X. M. Gao, M. W. Sigrist, E. Fertein, and W. D. Chen, Appl. Phys. Lett. **106**, 101109 (2015).

[5]S. Borri, P. Patimisco, I. Galli, D. Mazzotti, G. Giusfredi, N. Akikusa, M. Yamanishi, G. Scamarcio, P. De Natale, and V. Spagnolo, Appl. Phys. Lett. **104**, 091114 (2014).
[6]M. Mordmüller, M. Köhring, W. Schade, and U. Willer, Appl. Phys. B **119**, 111 (2015).
[7]Y. F. Ma, R. Lewicki, M. Razeghi, and F. K. Tittel, Opt. Express **21**, 1008 (2013).
[8]M. Köhring, S. Böttger, U. Willer, and W. Schade, Sensors **15**, 12092 (2015).
[9]W. Ren, W. Z. Jiang, N. P. Sanchez, P. Patimisco, V. Spagnolo, C. E. Zah, F. Xie, L. C. Hughes, R. J. Griffin, and F. K. Tittel, Appl. Phys. Lett. **104**, 041117 (2014).
[10]K. Liu, X. Y. Guo, H. M. Yi, W. D. Chen, W. J. Zhang, and X. M. Gao, Opt. Lett. **34**, 1594 (2009).
[11]L. Dong, V. Spagnolo, R. Lewicki, and F. K. Tittel, Opt. Express **19**, 24037 (2011).
[12]J. P. Waclawek, H. Moser, and B. Lendl, Opt. Express **24**, 6559 (2016).
[13]K. Liu, W. Zhao, L. Wang, T. Tan, G. Wang, W. Zhang, X. Gao, and W. Chen, Opt. Commun. **340**, 126 (2015).
[14]A. A. Kosterev, F. K. Tittel, D. V. Serebryakov, A. L. Malinovsky, and I. V. Morozov, Rev. Sci. Instrum. **76**, 043105 (2005).
[15]L. Dong, Y. J. Yu, C. G. Li, S. So, and F. K. Tittel, Opt. Express **23**, 19821 (2015).
[16]M. C. Wu, N. A. Olsson, D. Sivco, and A. Y. Cho, Appl. Phys. Lett. **56**, 221 (1990).
[17]M. Nakazawa, Y. Kimura, and K. Suzuki, Appl. Phys. Lett. **54**, 295 (1989).
[18]H. P. Wu, L. Dong, H. D. Zheng, X. L. Liu, X. K. Yin, W. G. Ma, L. Zhang, W. B. Yin, S. T. Jia, and F. K. Tittel, Sens. Actuators, B **221**, 666 (2015).
[19]H. P. Wu, A. Sampaolo, L. Dong, P. Patimisco, X. L. Liu, H. D. Zheng, X. K. Yin, W. G. Ma, L. Zhang, W. B. Yin, V. Spagnolo, S. T. Jia, and F. K. Tittel, Appl. Phys. Lett. **107**, 111104 (2015).
[20]S. Borri, P. Patimisco, A. Sampaolo, M. S. Vitiello, H. E. Beere, D. A. Ritchie, G. Scamarcio, and V. Spagnolo, Appl. Phys. Lett. **103**, 021105 (2013).
[21]S. T. Marshall, D. K. Schwartz, and J. W. Medlin, Sens. Actuators, B **136**, 315 (2009).
[22]K. L. Miller, E. Morrison, S. T. Marshall, and J. W. Medlin, Sens. Actuators, B **156**, 924 (2011).
[23]Z. Wang, Z. L. Li, and W. Ren, Opt. Express **24**, 4143 (2016).